



Mini-coil for magnetic stimulation in the behaving primate

Hadass Tischler^a, Shuki Wolfus^b, Alexander Friedman^b, Eli Perel^b, Tamar Pashut^a, Michal Lavidor^{a,c}, Alon Korngreen^{a,d}, Yosef Yeshurun^b, Izhar Bar-Gad^{a,d,*}

^a Gonda Multidisciplinary Brain Research Center, Bar Ilan University, Ramat Gan, Israel

^b Department of Physics, Bar Ilan University, Ramat Gan, Israel

^c Department of Psychology, Bar Ilan University, Ramat Gan, Israel

^d Goodman Faculty of Life Sciences, Bar Ilan University, Ramat Gan, Israel

ARTICLE INFO

Article history:

Received 12 June 2010

Received in revised form

28 September 2010

Accepted 15 October 2010

Keywords:

Transcranial magnetic stimulation (TMS)

Electrophysiology

Extracellular recording

Primate

Magnetic coil

ABSTRACT

Transcranial magnetic stimulation (TMS) is rapidly becoming a leading method in both cognitive neuroscience and clinical neurology. However, the cellular and network level effects of stimulation are still unclear and their study relies heavily on indirect physiological measurements in humans. Direct electrophysiological studies of the effect of magnetic stimulation on neuronal activity in behaving animals are severely limited by both the size of the stimulating coils, which affect large regions of the animal brain, and the large artifacts generated on the recording electrodes. We present a novel mini-coil which is specifically aimed at studying the neurophysiological mechanism of magnetic stimulation in behaving primates. The mini-coil fits into a chronic recording chamber and provides focal activation of brain areas while enabling simultaneous extracellular multi-electrode recordings. We present a comparison of this coil to a commercial coil based on the theoretical and recorded magnetic fields and induced electric fields they generate. Subsequently, we present the signal recorded in the behaving primate during stimulation and demonstrate the ability to extract the spike trains of multiple single units from each of the electrodes with minimal periods affected by the stimulus artifact (median period <2.5 ms). The directly recorded effect of the magnetic stimulation on cortical neurons is in line with peripheral recordings obtained in humans. This novel mini-coil is a key part of the infrastructure for studying the neurophysiological basis of magnetic stimulation, thereby enabling the development and testing of better magnetic stimulation tools and protocols for both neuroscientists and clinicians.

© 2010 Elsevier B.V. All rights reserved.

1. Introduction

Transcranial magnetic stimulation (TMS) is a non-invasive method of manipulating behavior by altering the underlying neuronal activity (Barker et al., 1985). This method is used extensively for both scientific (Walsh and Cowey, 2000; Pascual-Leone et al., 2000) and clinical (Pascual-Leone et al., 1996; Haraldsson et al., 2004) purposes. However, despite the dramatic rise in popularity of TMS over the last 25 years, its underlying effects on neuronal activity are to a large extent unknown. TMS has been shown to evoke a variety of responses depending on the stimulated site, stimulation intensity (Rizzo et al., 2004; Hanakawa et al., 2009) and stimulation frequency (Houdayer et al., 2008). Moreover, the effect seems to vary greatly depending on properties of the stimulation coil. Several different types of magnetic coils are commonly used including: circular coils, figure of 8 coils, butterfly shape coils and H coils (Cohen et al., 1990; Roth et al., 2007). Each of these coils exists in vari-

able coil sizes and configurations. Different geometries (shapes and sizes) of magnetic coils lead to different shapes and magnitudes of the magnetic field and the resulting induced electrical field (Cohen et al., 1990), leading to differences in the evoked neuronal activity and the resulting behavior. However, independently of their shape, all commercially available coils are designed for human brain stimulation and their sizes are customized for this purpose.

The direct (electrical) and indirect (synaptic) effects of TMS on the underlying tissue in the central nervous system (CNS) are poorly understood. Current evidence for stimulation-related changes in neuronal activity comes mostly from indirect measures. The evidence for neuronal effects ranges from purely behavioral changes to indirect physiological measures for the neuronal activity in the CNS. Indirect physiological measures do not directly assess neuronal firing in the CNS but rather are based on indirect correlates such as functional magnetic resonance imaging (fMRI) (Bohning et al., 1999; Ruff et al., 2009; Blankenburg et al., 2010) or positron emission tomography (PET) (Paus et al., 1997; Fox et al., 1997; Strafella et al., 2001). Another indirect method utilizes electrophysiological recordings in the muscles and peripheral nerves to assess the motor evoked potential (MEP) (Kammer et al., 2001; Hallett, 2007).

* Corresponding author at: Gonda Multidisciplinary Brain Research Center, Bar Ilan University, Ramat Gan 52900, Israel. Tel.: +972 3 5317141.

Direct recording of CNS neuronal activity has been obtained in humans during stereotactic neurosurgery using a single micro-electrode (Strafella et al., 2004). Recording during human surgeries has the enormous advantage of shedding light directly on the effects and mechanisms of TMS. However, such recordings are severely limited to studying the neurophysiological activity only in the clinically required targets and are also restricted by the duration and types of stimulation pulses possible during the operation. Direct recordings in the CNS of lab animals are severely limited by the dimensions of existing commercial “human-oriented” coils and their deleterious effects on neurophysiological recordings. A few studies have tested the effect of magnetic stimulation over the visual cortex in the cat on the local neuronal activity (Moliadze et al., 2003, 2005; de Labra et al., 2007; Allen et al., 2007; Pasley et al., 2009). The animal studies of magnetic stimulation effects utilize a standard human coil which generates a spatially huge magnetic field affecting a large portion of the animal (in this case: cat) brain relative to the fraction of the brain activated in humans. This limits the possibility of studying TMS effects on single functionally separate brain areas. Moreover, this method is limited in its applicability to behaving animals and to simultaneous multi-electrode recording in multiple brain areas.

Here we present a novel mini-coil which is specifically designed to enable multi-electrode recording in the CNS of behaving primates during magnetic stimulation. The coil design complies with the following stringent criteria: (1) the outer diameter of the coil must be small enough to fit into the recording chamber; (2) the inner diameter of the coil should be large enough to allow simultaneous electrode access to multiple brain structures; (3) the height of the coil must be limited to allow integration under the microdriving terminals; (4) the generated field should be equivalent to the one generated by standard “human-oriented” coils; (5) increases in temperature in the saline surrounding the coil (and thus the underlying tissue) should be limited to the physiological range. This coil has its own complementary hardware and software components which enable its seamless integration into standard multi-electrode extracellular recordings and the removal of stimulation artifacts. This infrastructure thus provides a setup for studying the underlying effect of TMS in both cognitive tasks and clinical states.

2. Methods

2.1. Coil fabrication

The design of the mini-coil was carried out using Vector Fields finite elements simulation (FES) software (Cobham Technical Services, Aurora, USA). Various coil configurations utilizing the short solenoid shape were simulated. The simulations enumerated over wire diameter, coil diameter and coil height while adhering to the physical constraints. A “wet-winding” method was used for winding a standard lacquer insulated copper wire (1.15 mm diameter). A low viscosity Epoxy EP29LPSP compound (Master Bond Inc., Hackensack, USA), mixed with 25 μm fine Alumina particles were used to impregnate the coil during the winding process. Alumina particles were added (at a weight ratio of 7 g Alumina to 5 g Epoxy) for coil reinforcement as well as for improved electrical insulation and heat transfer (Friedman et al., 2006). The coil itself is mandrel-free due to space constraints and is attached to its support connecting to the measurement chamber using EP51 fast curing Epoxy (Master Bond Inc., Hackensack, USA). Small wire bending diameters were avoided to prevent hot spots of high electric fields. The electrical insulation of the coil and its windings is of crucial importance for the development of mini-coils as the coil is immersed in saline and prone to electrical breakdown to

the solution. Our innovative insulation method makes it possible to use such mini-TMS coils when in contact with extracellular solution and was tested to voltage levels up to 1200 V. A 0.1 mm thick grounded copper sheet, cut to prevent major eddy current loops, covers the surface of the coil to minimize capacitance effects between the coil and the saline. Finally, a Pt100 temperature sensor is attached to the surface of the coil in contact with the solution to monitor the temperature. This allows for the definition of pre-defined temperature limits which can halt the experiment in the case of possible overheating of the underlying brain tissue.

2.2. Power supply

A high-voltage DC power supply (HCK 400–2000, FuG Elektronik, Rosenheim, Germany) was used to charge a custom made capacitor array (adjustable 50–200 μF). A custom made control unit guaranteed that the output of the system was disconnected from the coil during the capacitor charging process and between the pulses. A bi-modal full wave cycle was generated by the system with a time constant which was derived from the capacitance and inductance of the system. The time constant in our system was selected to resemble the one used by commercial human TMS systems. The coil cannot currently be operated by the power unit of conventional TMS systems, since: (1) the coil parameters (such as inductance and resistance) are different from commercial coils; (2) our system allows greater flexibility as regards the stimulus parameters such as the time constant, voltage, pulse shape, etc. The schematics for the control unit are available to other investigators upon request.

2.3. Magnetic field

The magnetic field was assessed using Finite Element Analysis (FEA) for magnetic field modeling. FEA is a numerical technique for finding approximate solutions to partial differential equations (PDE) as well as integral equations. The solution approach is based either on eliminating the differential equation completely (steady state problems), or rendering the PDE into an approximating system of ordinary differential equations, which are then numerically integrated using standard techniques such as Euler’s method or Runge–Kutta. FEA was carried out using Vector Fields PC Opera finite element software. The spatial distribution of the actual magnetic fields generated by the mini-coil and the human coil used for control were measured by feeding DC current into the coil and recording the parallel magnetic field component along the coil central axis using LakeShore’s model 410 Gaussmeter (Lake Shore Cryotronics Inc., Westerville, USA). The sensor active area was approximately 1 mm^2 , and the measured field resolution was 10^{-5} T. Comparison of all the results was made to a commercially available 50/110 mm internal/external diameter round coil which was activated using a 2000 Super Rapid Magnetic Stimulator (Magstim, Dyfed, UK).

2.4. Induced electric field

The electric field was calculated using MATLAB (MATLAB 2007B, Mathworks, Natick, MA, USA). The field was calculated for a slice at a fixed distance (z) from the coil using a superposition of the fields induced by each of the loops making up the coil. For each loop we used the prior formulation (Tofts, 1990):

$$\vec{A} = \frac{\mu_0 I}{\pi k} \left(\frac{r}{x} \right)^{1/2} \left[K(m) \left(1 - \frac{1}{2} k^2 \right) - E(m) \right] \hat{\theta} \quad (1)$$

$$m = k^2 = \frac{4rx}{(r+x)^2 + z^2} \quad (2)$$

where \vec{A} is the vector potential for a single loop, μ_0 is the permeability constant, I is the current, r is the loop radius, z is the distance of the point from the loop plane, x is the distance of the point from the center of the coil, $K(m)$ and $E(m)$ are elliptic integrals of the first and second order and $\hat{\theta}$ is the unit vector in the direction θ . This was derived to calculate the contribution of a single loop to the induced electric field:

$$\vec{E} = -\frac{\partial I}{\partial t} \frac{\mu_0}{\pi k} \left(\frac{r}{x}\right)^{1/2} [K(m)(1 - \frac{1}{2}k^2) - E(m)] \hat{\theta} \quad (3)$$

2.5. Electrophysiological recordings

The neuronal recordings were taken from an awake behaving Cynomolgus monkey (*Macaca fascicularis*, male, 4 kg). All procedures were in accordance with the National Institutes of Health Guide for the Care and Use of Laboratory Animals and Bar-Ilan University Guidelines for the Use and Care of Laboratory Animals in Research and were approved and supervised by the Institutional Animal Care and Use Committee (IACUC). The monkey's condition was monitored carefully online via visual inspection and offline using video inspection to detect any signs of discomfort due to the magnetic stimulation. The monkey (and two other monkeys on which the coil was used) did not display any signs of discomfort due to the stimulation and was able to behave normally and perform simple sensory-motor tasks without evident problem. Full details of a similar experimental protocol appear elsewhere (Erez et al., 2009). Briefly, data were acquired via multiple micro-electrodes extended to the motor cortex and different nuclei of the basal ganglia through a 27 mm square Cilux recording chamber (Alpha–Omega Engineering, Nazareth, Israel). The mini-coil was attached to the microdriving terminal (MT) which was also used for positioning the micro-electrodes. Extracellular recording was performed via eight glass-coated tungsten micro-electrodes (impedance, 0.25–0.7 M Ω at 1 kHz). The electrode signal was amplified with a gain of 1000 and bandpass filtered with a 2–8000 Hz four-pole Butterworth filter (MCP+ 4.10, Alpha–Omega Engineering). The signal was continuously sampled at 40 kHz with 14-bit resolution (AlphaMap 10.10, Alpha–Omega Engineering).

2.6. Artifact removal

The magnetic stimulation results in the formation of a significant electrical artifact on the recording electrodes. Minimizing the duration in which the artifact masks the neuronal activity is crucial for successfully identifying rapid (short-latency) neuronal responses to the stimulation. This was done by making hardware changes such as advanced grounding, wide band filtering combined with low amplification, and applying offline artifact removal performed in software. Artifact removal was done using our custom developed Stimulus Artifact Removal Graphical Environment (SARGE) (Erez et al., 2010) written in MATLAB (MATLAB 2007B, Mathworks, Natick, MA). This framework allows high flexibility in dealing with artifacts which vary greatly in their characteristics, as is typical of magnetic stimulation. The neuronal activity during the saturation is lost; however, neuronal activity following that period may be reconstructed. Periods of stable artifact following the magnetic stimulation were typically removed using a moving mean shape subtraction whereas unstable responses were handled using a single pulse polynomial fit of the artifact (Erez et al., 2010).

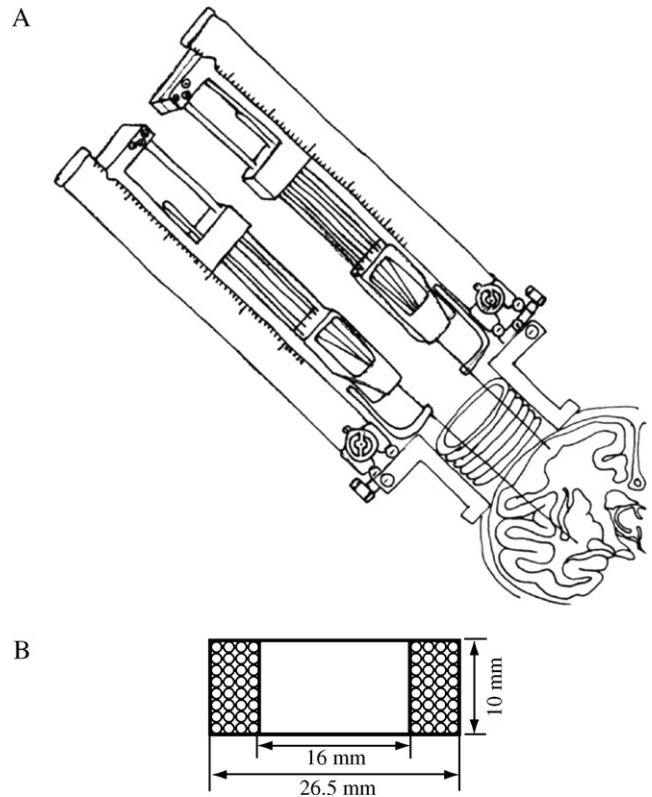


Fig. 1. Mini-coil architecture. (A) A sketch of the mini-coil located inside the recording chamber and attached to the multi-electrode double microdriving terminal. (B) Schematic drawing of a cut through the mini-coil.

3. Results

3.1. Coil architecture

The mini-coil was designed to provide a magnetic pulse which generates a field intensity comparable to commercial TMS stimulators, namely on the order of 1 T with 400 μ s duration. The mini-coil had to match the stringent constraints of the standard primate recording chamber size which limits both its outer diameter and height. Moreover, to accommodate for the in vivo multi-electrode recording performed during stimulation, the inner diameter was maximized to allow optimal electrode manipulation enabling access to different brain structures which require different entry coordinates. The close proximity of the dura of the animal resulted in another constraint on increases in temperature in the saline surrounding the mini-coil which had to be limited to a narrow physiological range. The circular coil was attached to the electrode microdriving terminal which enabled separate insertion of multiple micro-electrodes into different brain regions. The whole complex was then attached to the recording chamber with the coil situated completely within the chamber (Fig. 1A). The exact position of the coil from underneath the microdriving terminal (MT) may be changed with sub-millimeter resolution enabling variable distances from the underlying dura. This configuration verifies a perpendicular trajectory of the electrodes relative to the mini-coil, thereby minimizing the electrical currents and the resulting stimulation artifacts generated on them. This also enables a fixed location of the coil over the cortex, thus reducing the variability of the stimulation location which is typical of standard coils. Following FES modeling, the optimized coil configuration was selected to be a short solenoid shape with the following parameters: outer diameter 26.5 mm, inner diameter 16 mm, coil height 10 mm, wire diameter 1.2 mm, number of turns 32 (Fig. 1B). This compares to

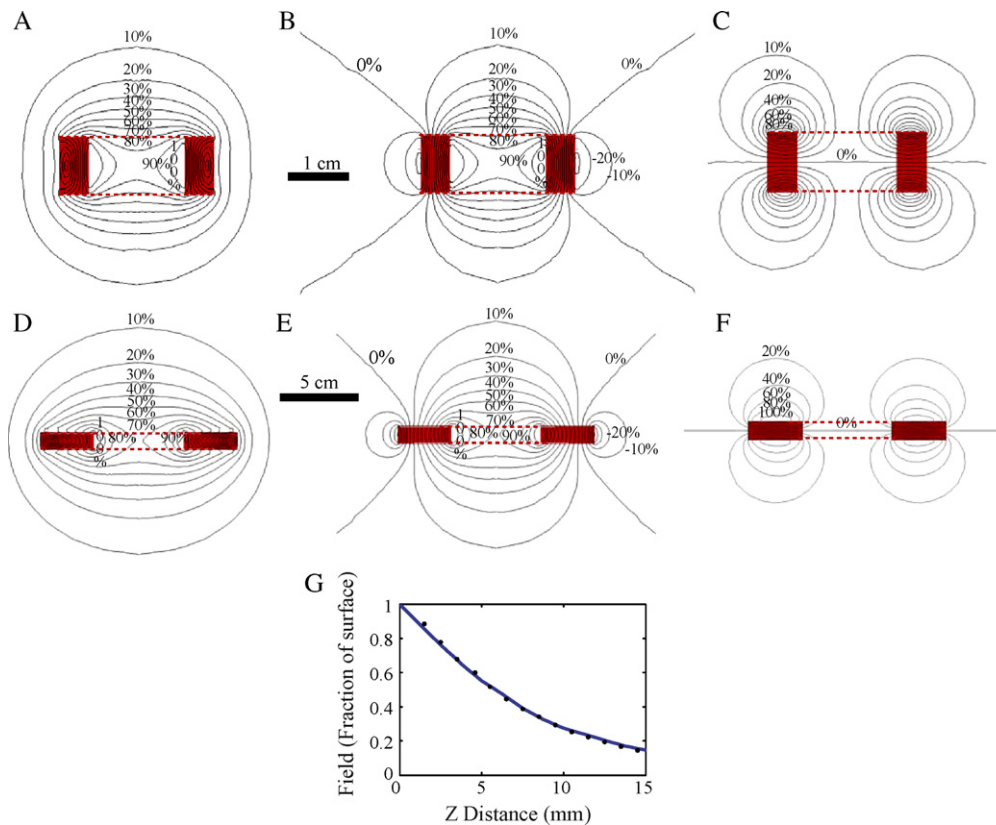


Fig. 2. Distribution of the magnetic field. Distribution of the magnetic field of the (A–C) mini-coil and (D–F) a human circular (5/11 cm internal/external diameter) coil. Different properties of the field are shown: (A, D) absolute value of the field vector (B). (B, E) The magnetic field component parallel to the coil central axis (B_z) and (C, F) the magnetic field along the coil (B_r). (G) Theoretical (solid line) and recorded (dots) field dependence on distance (z) of the mini-coil.

a standard coil (Magstim, Dyfed, UK) which is roughly four times larger in diameter with an outer diameter of 110 mm, an inner diameter of 50 mm and a coil height of 12 mm.

3.2. Magnetic field

Magnetic field modeling using FES was used to assess the field surrounding the coil. The model assumes homogenous current density within the conducting space (gray regions in Fig. 2A–F). The magnitude of the magnetic field (B) of the mini-coil is shown relative to the maximal value (Fig. 2A). The direction of the field is shown using the magnetic field component parallel to the coil central axis (B_z) (Fig. 2B) and the radial component of the magnetic field (B_r) (Fig. 2C). The contour lines in the figures connect points of equal field values. Equivalent calculations were made for the commercial human coil for comparison (Fig. 2D–F respectively). As is typical of short solenoid coils, the field of the mini-coil drops sharply with increasing distance from the coil. Thus, neuronal tissue located 5 mm below the coil surface will be exposed to roughly half of the field immediately following the surface of the winding. The spatial distribution of the magnetic field was measured experimentally using a Gaussmeter. The recorded B_z data normalized to the value at the coil surface was compared to the finite element modeling values of the coil (Fig. 2G). The theoretical and recorded values of the magnetic field are for the coils in air.

3.3. Induced electric field

The induced electric field (E) was directly calculated for both coils in air. The electric fields for both the mini-coil and the commercial human coil had maximal values in the area under the coil

itself which decayed both towards the center of the coil and the external surrounding areas. The induced electric field is shown for a plane which represents to distance (along the z axis) of the coil surface from the cortex, 2 mm in the mini-coil (Fig. 3A) and 15 mm (McConnell et al., 2001) in the commercial coil (Fig. 3B). The induced electric field depends on the magnetic field and the radius of the coil. Thus, for the same magnetic field ($B = 1$ T in the center of the coil) the maximal electric field is larger in the commercial coil. However, the region of interest in the primate is small and falls within the mini-coil diameter. In this region the electric field of both coils with the same magnetic field is roughly similar (Fig. 3C). The decay of the electric field over the distance from the surface is rapid compared to the commercial coil (Fig. 3D). This is a useful property of the coil as its surface is dramatically closer to the cortex (2 mm compared to 15 mm) and the underlying primate brain is smaller than the human brain.

3.4. Magnetic pulse

The shape and magnitude of the magnetic pulse was measured for the mini-coil and the commercial TMS coil. The discharge through the mini-coil was normalized so that the maximal voltage of the capacitor charge (1200 V) was defined as 100% of the mini-coil output. A pickup coil (10 mm diameter) was used for recording the time dependent voltage induced in the loop following a magnetic pulse through the freestanding mini-coil (Fig. 4A). The magnetic pulse shape and amplitude were then calculated using time-integration over the recorded signal and the necessary geometry and calibration factors. The pickup coil was calibrated against a known magnetic field pulse. Identical magnetic pulse calculations were performed for the mini-coil (Fig. 4B) and the commercial TMS

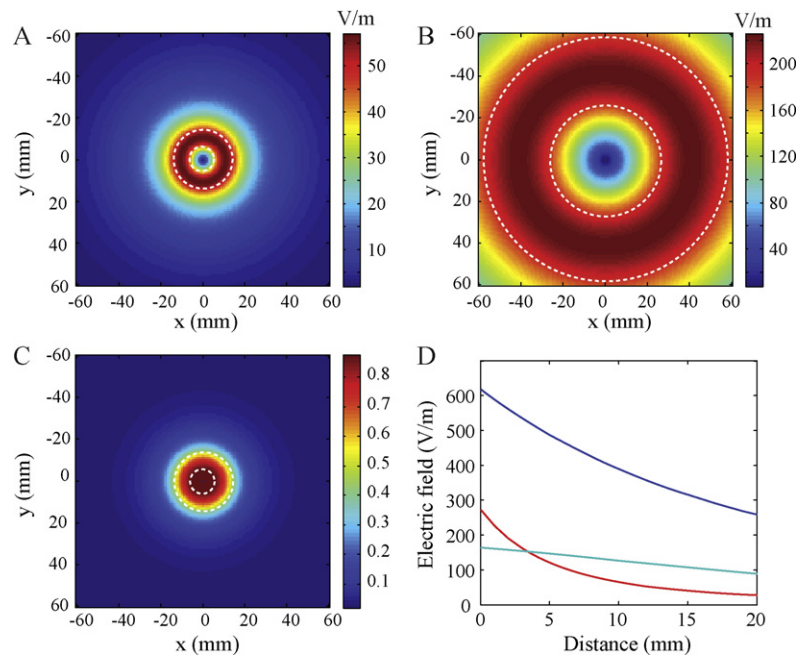


Fig. 3. Distribution of the induced electric field. (A, B) The calculated electric field for $B=1\text{ T}$ at the center of the coil shown along the x - y axis (A) beneath the mini-coil at $z=2\text{ mm}$, and (B) beneath the commercial coil at a $z=15\text{ mm}$. (C) Ratio of the field along the x - y axis between the mini-coil and the commercial coil. The dotted white lines mark the inner and outer diameters of the (A & C) mini-coil and (B) commercial coil. (D) Decay of the maximal electric field (100% stimulator intensity) of the mini-coil (red) and commercial coil (dark blue) and the maximal electric field of the commercial coil within the diameter of the mini-coil (light blue) over z . (For interpretation of the references to color in this figure legend, the reader is referred to the web version of the article.)

coil (Fig. 4C). In both cases the recording was along the central axis of the coil, right at its edge. The results demonstrate that the mini-coil generates a magnetic pulse similar in shape and period ($\sim 400\ \mu\text{s}$) to the extensively used commercial TMS systems. Furthermore, the maximal magnetic field intensity of the mini-coil can be tuned to match and exceed that of the commercial TMS instrument. A stimulation pulse generated after the capacitor was charged at 600 V (50% of the maximal output) led to the formation of a magnetic field with a maximal intensity of $>1.5\text{ T}$ at the coil center, which exceeds the peak intensity obtained under full power stimulation of this commercial TMS. The maximal power (1200 V) of the mini-coil system enables the generation of a maximal magnetic field far larger than the maximal field of current commercial systems (Rossini et al., 1994). A stimulation pulse generated after the capacitor charged at 600 V typically elicited movement (supra motor threshold stimulation) while a pulse following charging at 400 V typically did not elicit movement (sub motor threshold stimulation). The pulse amplitude required for eliciting movement did not change as a function of the chamber conductivity i.e. air or saline filled.

3.5. Heating

The large currents flowing through the coil lead to its heating due to its resistance. This heat dissipates through the surrounding saline to the dura and from there to the underlying neuronal tissues. Assessment of heating during repetitive magnetic pulses was performed, for safety reasons, in an *in vitro* study within a chamber similar to the one typically attached to the primate during the *in vivo* experiment. The chamber is square based (27 mm^3) with a volume of 13 cm^3 . The coil itself has a volume of 4 cm^3 , leaving an approximate space of 9 cm^3 for the saline filling the chamber. The temperatures were recorded using a Pt100 temperature sensor attached to the coil itself over a period of 5 min during stimulation at rates of 0.2–1 Hz and at voltages around the motor threshold: sub-threshold at 400 V (33% of maximal stimulator power) and

supra-threshold at 600 V (50% of maximal stimulator power). The heating of the coil from room temperature (24°C), which mimics the standard procedure of chamber filling prior to session initiation, did not exceed safe temperature values at 0.5 Hz using supra-threshold voltage (600 V) and at 1 Hz using sub-threshold voltage (400 V) (Fig. 5A). Similar recordings were performed using saline at the initial animal body temperature (36°C) and led to comparable results (Fig. 5B). Higher frequency stimulation required for some rTMS protocols requires a different approach which involves using a slow saline flow through the chamber via a standard peristaltic pump (Masterflex L/S, Cole Parmer, Vernon Hills, IL, USA). The saline flow is achieved by using two tubes connected to the same pump for concurrent inward and outward flow, maintaining a constant saline level in the chamber. The heating was tested using a room temperature saline flow of either 10 ml/min or 30 ml/min (Fig. 5C) enabling a protocol of up to 2 Hz for prolonged periods. The graphs provide an upper-bound to the heating process as it does not include the additional significant heat dissipation occurring in the *in vivo* state due to heat transfer to the neural tissue and its dissipation through the cerebrospinal fluid (CSF) and blood flow.

3.6. Electrophysiological recordings

The magnetic pulses generated large electrical artifacts on the recording micro-electrodes. These artifacts were further distorted by the amplification and filtration performed by multiple hardware components leading from the electrode to the acquisition system. Using low amplification and a wide band filtration scheme these distortions were minimized but are still huge compared to the typically sub-millivolt extracellular spikes. The artifacts were further reduced by enforcing a perpendicular entry of the electrodes relative to the coil, thus minimizing their direct field exposure. The resulting signal was then processed offline to remove the artifact, leaving the neuronal signal reflecting the stimulation effect on the neuronal activity but without the direct effect of the stimulation

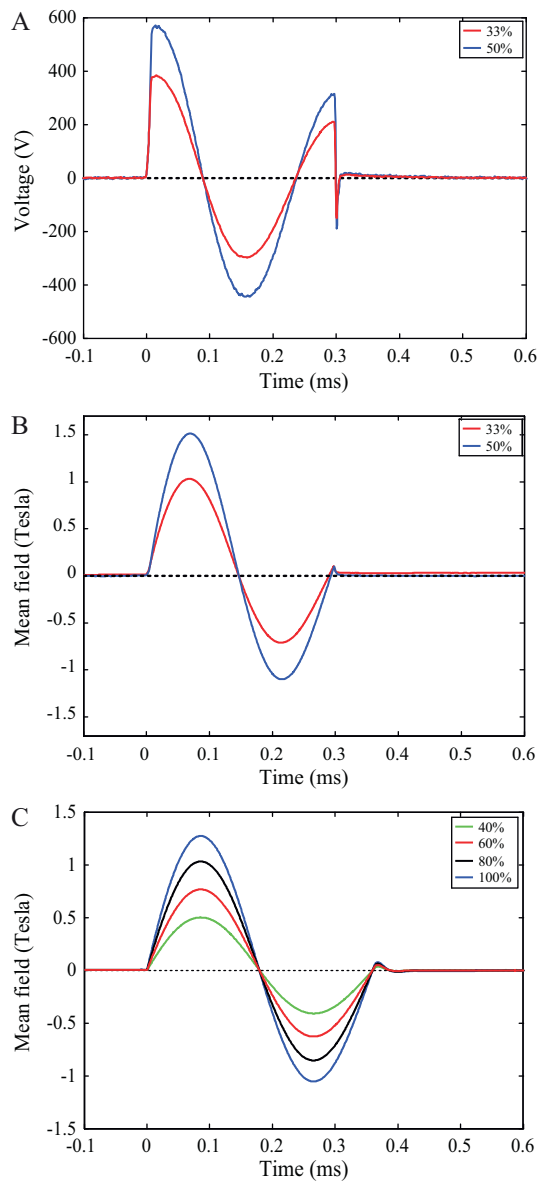


Fig. 4. Magnetic pulse shape. (A) Voltage pulse over the mini-coil at different capacitor charging voltages. (B) Field generated by the mini-coil at the center of the coil and at distance 0 from its edge at different capacitor charging voltages. (C) Field generated by the human coil (round 5/11 cm internal/external diameter) at the center of the coil and at distance 0 from its edge at different percentage of maximal charging voltage.

pulse. The artifact removal process included a multistage signal reconstruction process in the SARGE framework (Erez et al., 2010). The process included identification of stimulation events, definition of saturation periods and removal of the rest of the artifact using either removal of a moving average shape or removal of a polynomial regressed to fit the artifact (Fig. 6). The process led to the reconstruction of the original signal with a loss of a few milliseconds due to the saturation (median dead time 2.5 ms, $n = 330$). This allowed for a reconstruction of the neuronal response to the stimulation on a fine temporal scale which lost only the direct (non-synaptic) responses which are typically in or under the millisecond scale. The vastly different shapes of the artifact stimulus across electrodes may be seen in the traces of multiple electrodes recorded together (Fig. 7A); thus the artifact removal information was not utilized across electrodes. However, the artifact suppression infrastructure enables generating a clean signal with minimal

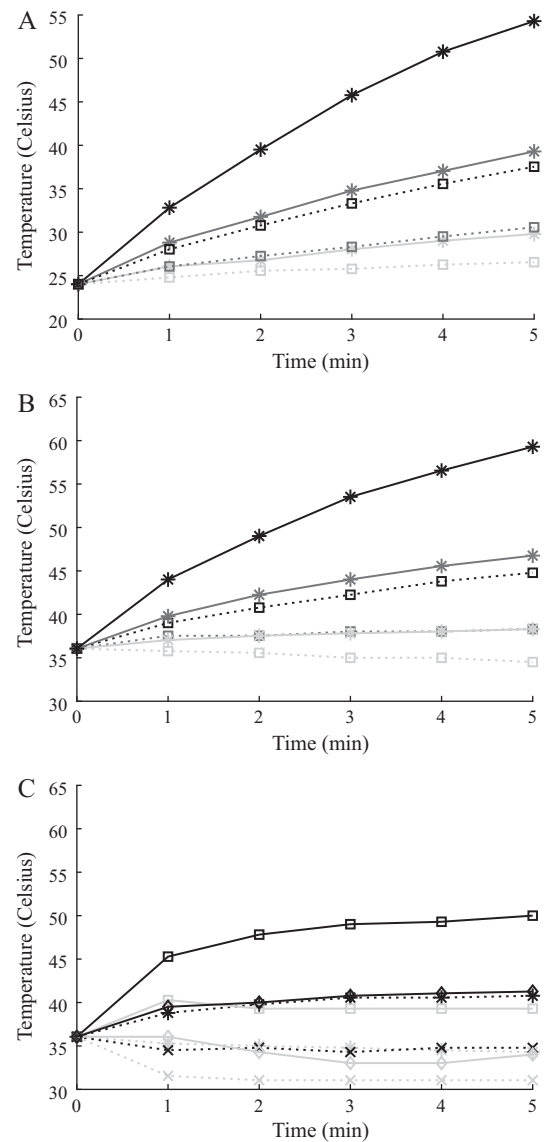


Fig. 5. Heating of the mini-coil. Temperature change of the mini-coil during repetitive pulsed stimulation performed in a chamber filled with saline. (A, B) Changes during stimulation in the frequency range of 0.2, 0.5 and 1 Hz (light grey, dark grey and black respectively) and using supra-threshold (50%) and sub-threshold (33%) of the maximal discharge output (solid lines with asterisk markers and dotted lines with square markers respectively) using initial (A) room temperature (24 °C) or (B) body temperature (36 °C). (C) Changes during stimulation of 1 Hz (grey) and 2 Hz (black) using supra-threshold (50%) and sub-threshold (33%) of the maximal discharge output (solid lines and dotted lines respectively) employing saline circulation within the chamber at a rate of either 10 ml/min (square and asterisk) or 30 ml/min (diamond and x shape).

artifact across all electrodes (Erez et al., 2010) thus enabling, for the first time, the simultaneous recording of multiple extracellular signals within different parts of the brain during magnetic stimulation (Fig. 7B).

The signals were offline sorted to extract multiple single unit activities. The typical neuronal activity in the primary motor cortex (M1) fit the results recorded in the periphery following stimulation. During supra motor-threshold stimulation the neuron responded with a short latency locked activation and a prolonged inhibition followed in some cases by rebound excitation periods (Fig. 8A and B). The cross trial variability, expected from the single units may be seen in the peri-event raster. However, the summation of all trials demonstrated the classical response reflected in the peri-stimulus histogram (PSTH). The neuron was not activated dur-

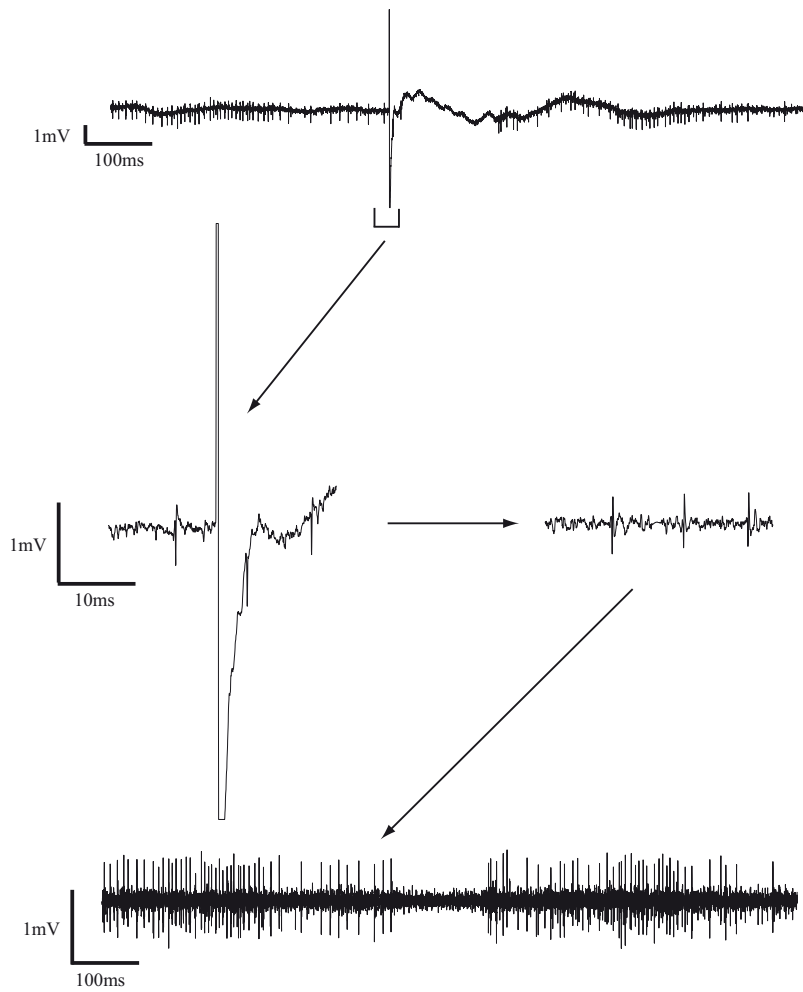


Fig. 6. Stimulation artifact. (Top) Example of an electrophysiological recording in the primary motor cortex (M1) demonstrating the stimulus artifact resulting from the magnetic pulse. (Center, left) The detailed shape of the stimulus artifact exceeding the amplitude of the neuronal spikes by multiple factors. (Center, right) The stimulus artifact is removed using a subtraction of the mean shape leaving an artifact free signal. (Bottom) Same example as shown above after the removal of the artifact demonstrating the inhibition of the neuronal firing of the stimulated cortical neuron.

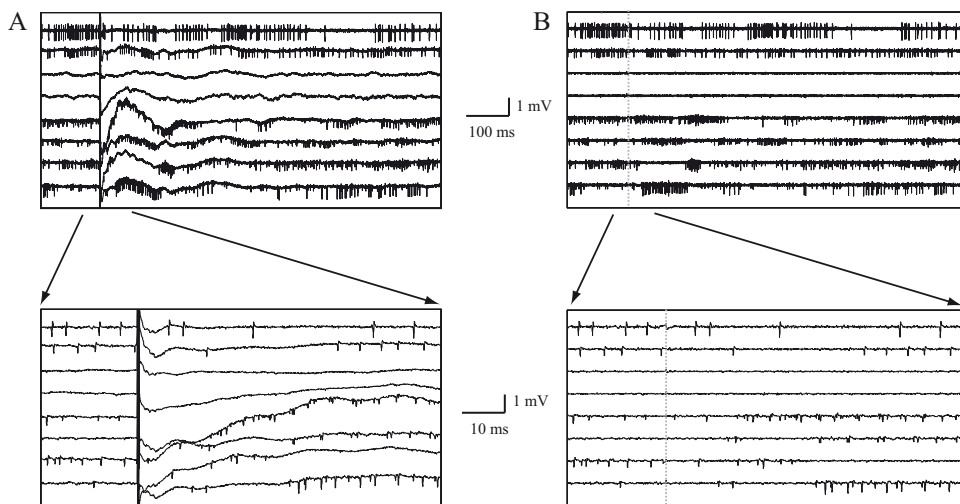


Fig. 7. Multi-electrode recording. An example of a simultaneous recording from eight electrodes located in different brain areas (cortex and basal ganglia). (A) The raw recorded signals and the (B) same signal after artifact removal are shown in two time scales, (top) 1 s window and (bottom) 100 ms window surrounding the magnetic stimulation pulse.

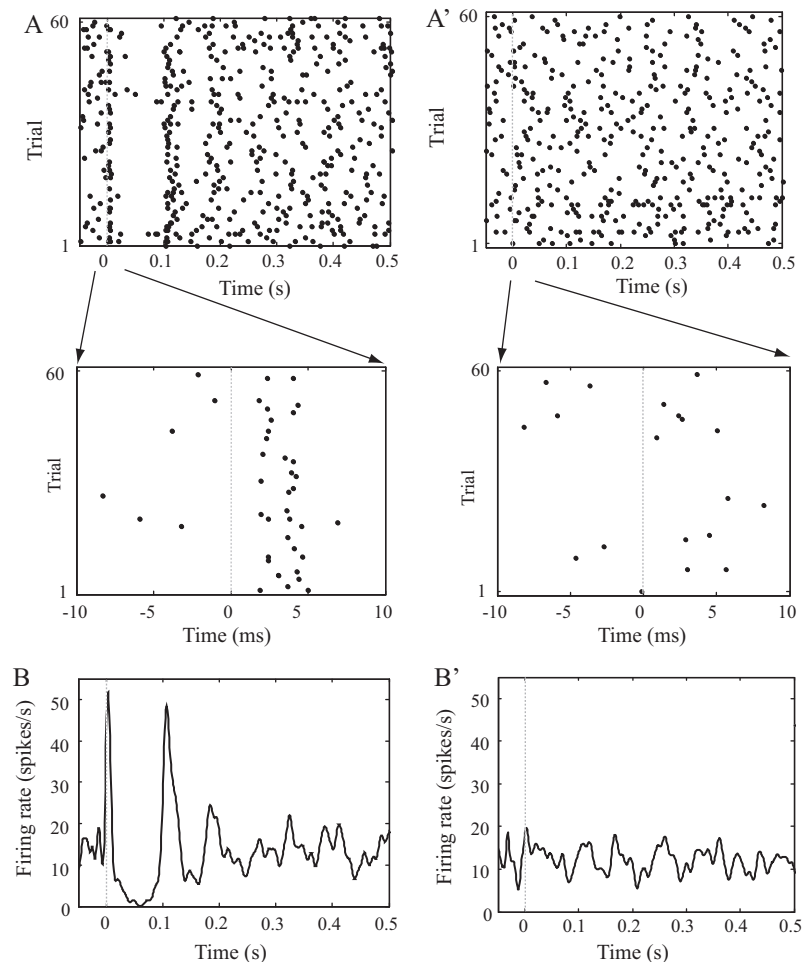


Fig. 8. Cortical response to stimulation. An example of the response of a cortical (M1) neuron to magnetic stimulation. The peri-event rasters of the neuronal activity surrounding the (A) supra motor threshold and (A') sub motor threshold are shown on two time scales spanning (top) 0.6 s and (bottom) 0.02 s demonstrating the locking to the stimulation as early as 2 ms following the stimulation. The peri-stimulus histogram (PSTH) is shown for the same neuron using the same stimuli intensities (B and B' respectively).

ing sub motor threshold stimulation as is evident by observing the raster and histogram (Fig. 8A' and B').

4. Discussion

The mini-coil was developed to meet the stringent requirements of enabling simultaneous magnetic stimulation and multi-electrode extracellular recording in the behaving primate. These requirements determined the physical dimensions of the coil, derived from the recording chamber size, the coil shape, derived from the integration into the electrode manipulation towers, and finally the required magnetic field, derived from the smaller size of the primate brain and the shorter distance to the cortex inside the chamber. The derived coil size is 26 mm × 10 mm and generates magnetic fields which may exceed 3 T over short distances, enabling focal activation of the primate cortex with a two-fold decrease in the field over each 5 mm. The magnetic pulse, which has the same shape as the one used in commercial TMS coils, leads to muscle activation at ~400 V and allows scaling up to significantly larger fields. The coil enables the administration of prolonged repetitive TMS (rTMS) protocols while controlling for temperature changes in the saline surrounding the coil. Finally, neurophysiological experiments performed using this coil showed a safe usage of the coil in a behaving primate demonstrating continuous recording using multiple independent channels and the removal of magnetic pulse artifacts with dead times of 2.5 ms enabling the reconstruc-

tion of neuronal activity occurring in close temporal proximity to the stimulation pulses.

Research on the effects of magnetic activity on neuronal activity requires an animal model study of the basic mechanisms. However, the human brain is physically larger than the animal brain; for example the volume of the human brain is roughly 15 times larger than the Macaque brain (Rilling and Insel, 1999). Moreover, the size of functionally discrete cortical areas (such as M1) in the human is much larger. The activation of the neurons in the underlying tissue depends on the induced electric field (E) rather than the magnetic field (B). The maximal induced electric field, determined by the magnetic field and the radius of the coil, is larger in larger coils with equal magnetic fields. The magnetic field of the mini-coil was designed to be comparable with the commercial coil at the coil center. Thus, the electric field of both coils is comparable up to the radius of the mini-coil. From that distance on, the electric field of the mini-coil decreases while that of the larger commercial coil keeps increasing. Therefore, the electric field generated by both coils at the region of interest in our experiments (beneath the mini-coil) is comparable for both coils. Multiple methods of generating a more focal magnetic field exist, most notably the figure of 8 coils. These coils, which are physically much larger than our mini-coil, make it possible to achieve a comparable focal shape of the magnetic field. However, a circular coil enables simple insertion and manipulation of multiple electrodes into the brain, thus maintaining its usage requirements following its miniaturization. It is important to note

that the mini-coil, like all magnetic stimulation coils in general and specifically round coils, is far from reaching the focality of electrical stimulation methods. Thus, additional cortical areas may be activated, both directly and indirectly, when attempting to stimulate the desired cortical region. Moreover, the shape of the field leads to differential stimulation of neurons within different cortical areas which are located in different parts of the chamber. Some cortical neurons are activated directly by the coil, others are activated only synaptically, while still others are not activated at all. Recordings during the stimulation may be performed in any of these cortical areas. Furthermore, studies of sub-cortical areas which are activated only indirectly (synaptically) may be performed using this mini-coil setup.

The mini-coil diameter is less than a quarter of the human coil diameter, which leads to changes in its magnetic field and induced electric field properties. The rapid decay of the field over distance due to its smaller diameter is compensated for by the ability to bring the coil closer to the cortex (typically <1 mm from the dura) which allows activation of the cortex at relatively small voltages. Moreover, this rapid decay of the field is crucial to guarantee that only cortical structures are activated in a way comparable to the stimulation created using regular coils in humans. These standard coils have slower decay over space and will thus affect deep structures in the smaller brains of animals, thus leading to different response mechanisms from the ones activated in humans.

Historically, assessments of the effects of magnetic stimulation of the brain have been based on either recording in the periphery, primarily motor evoked potentials (MEPs) to reveal motor cortex activation (Fitzgerald et al., 2002) or by comparison to electrical stimulation (Krnjevic et al., 1966; Day et al., 1989) which is technically easier to study. However, both of these methods do not provide a direct way of quantifying neuronal activity. Recently neurophysiological recordings were made in the visual cortex of the anesthetized cat (Moliadze et al., 2003, 2005; de Labra et al., 2007; Allen et al., 2007; Pasley et al., 2009). This method is limited in its application to behaving animals and to its usage with multiple electrodes in different brain areas. Moreover, the usage of the human coil over the significantly smaller animal brain results in a much larger distribution of the field over the brain, impeding the study of TMS effects on a functionally separate brain area in the animal. One study was carried out in humans during stereotactic neurosurgery while applying magnetic stimulation over the primary motor cortex (M1) and recording in the subthalamic nucleus (STN) using single micro-electrode (Strafella et al., 2004). Recording during human surgeries has the advantage of examining the effect and mechanism of TMS directly. However, such recordings are typically limited in the location and electrodes to the clinically relevant location and other areas en-route to the final target. In addition, the operating room is a non-optimal neurophysiological recording environment because of the increased electro-magnetic noise and reduced grounding and shielding. This leads to increased amplification and narrower filtering, resulting in recordings which suffer from prolonged stimulation induced artifacts that last typically for ~8 ms (Strafella et al., 2004) compared to the shorter (~2.5 ms) artifacts using the mini-coil which thereby enables the detection of short latency responses to the stimulation.

Alongside with the advantages provided by the mini-coil, this unique setup presents several limitations which should be taken into account when it is used for studying magnetic stimulation: (1) the location of the coil is fixed within the chamber; this has the advantage of providing a reproducible stimulation but severely limits the ability to stimulate multiple brain areas or refine the location after the chamber implantation. This highlights the importance of chamber location planning prior to surgery and its placement during surgery for optimal stimulation results; (2) the coil is smaller than human commercial coils; however, like all round coils it is limited

in its focality and may directly activate cortical areas which are outside of the chosen area; (3) the large currents flowing through the coil cause it to heat. As the coil may not be removed during the stimulation session the number and frequency of pulses must be limited or alternatively a saline circulation system must be installed to allow longer higher frequency protocols. Large temperature changes within the chamber may lead to direct temperature derived modulation of neuronal activity (due to either cooling or overheating of the neuronal tissue). This may be controlled by a circulation system using either an open loop (manual setting of the flow rate for each stimulation protocol) or closed loop (automatic setting of the flow rate using the input from the temperature sensor on the coil) solutions.

Overall, the mini-coil provides a unique tool for the study of neuronal activity in response to magnetic stimuli. The coil enables recording in awake behaving primates through multiple (up to 16 in our setup) electrodes which may be situated in different brain structures. Moreover, the coil is part of an infrastructure which allows for the examination of the derived signal with minimal stimulation artifacts. The coil provides a significant improvement in focal activation of the primate brain using magnetic fields comparable to the much bigger human coils, thus providing activation of comparable functionally distinct brain areas. This provides a unique model for studying the effect of TMS in lab animals and provides insights into the mechanisms behind this important clinical and research tool.

Acknowledgments

This work was supported by an ISF Converging Technologies Grant (1698-07). We thank M. Abeles for his advice, M. Israelashvili and U. Berger for help with the measurements, K. Belevsky and M. Dror for their help with the animal surgery and maintenance and D. Nesselroth for help with the graphics.

References

- Allen EA, Pasley BN, Duong T, Freeman RD. Transcranial magnetic stimulation elicits coupled neural and hemodynamic consequences. *Science* 2007;317:1918–21.
- Barker AT, Jalinous R, Freeston IL. Non-invasive magnetic stimulation of human motor cortex. *Lancet* 1985;1:1106–7.
- Blankenburg F, Ruff CC, Bestmann S, Bjoertomt O, Josephs O, Deichmann R, et al. Studying the role of human parietal cortex in visuospatial attention with concurrent TMS–fMRI. *Cereb Cortex* 2010.
- Bohning DE, Shastri A, McConnell KA, Nahas Z, Lorberbaum JP, Roberts DR, et al. A combined TMS/fMRI study of intensity-dependent TMS over motor cortex. *Biol Psychiatry* 1999;45:385–94.
- Cohen LG, Roth BJ, Nilsson J, Dang N, Panizza M, Bandinelli S, et al. Effects of coil design on delivery of focal magnetic stimulation. Technical considerations. *Electroencephalogr Clin Neurophysiol* 1990;75:350–7.
- Day BL, Dressler D, Maertens de NA, Marsden CD, Nakashima K, Rothwell JC, et al. Electric and magnetic stimulation of human motor cortex: surface EMG and single motor unit responses. *J Physiol* 1989;412:449–73.
- de Labra C, Rivadulla C, Grieve K, Marino J, Espinosa N, Cudeiro J. Changes in visual responses in the feline dLGN: selective thalamic suppression induced by transcranial magnetic stimulation of V1. *Cereb Cortex* 2007;17:1376–85.
- Erez Y, Czitron H, McCairn K, Belevsky K, Bar-Gad I. Short-term depression of synaptic transmission during stimulation in the globus pallidus of 1-methyl-4-phenyl-1,2,3,6-tetrahydropyridine-treated primates. *J Neurosci* 2009;29:7797–802.
- Erez Y, Tischler H, Moran A, Bar-Gad I. Generalized framework for stimulus artifact removal. *J Neurosci Methods* 2010;191:45–59.
- Fitzgerald PB, Brown TL, Daskalakis ZJ, Chen R, Kulkarni J. Intensity-dependent effects of 1 Hz rTMS on human corticospinal excitability. *Clin Neurophysiol* 2002;113:1136–41.
- Fox P, Ingham R, George MS, Mayberg H, Ingham J, Roby J, et al. Imaging human intra-cerebral connectivity by PET during TMS. *Neuroreport* 1997;8:2787–91.
- Friedman A, Wolfus S, Yeshurun Y, Bar-Haim Z. Method for manufacturing superconducting coils. US Patent 2006/0071,747; 2006.
- Hallett M. Transcranial magnetic stimulation: a primer. *Neuron* 2007;55:187–99.
- Hanakawa T, Mima T, Matsumoto R, Abe M, Inouchi M, Urayama S, et al. Stimulus-response profile during single-pulse transcranial magnetic stimulation to the primary motor cortex. *Cereb Cortex* 2009;19:2605–15.
- Haraldsson HM, Ferrarelli F, Kalin NH, Tononi G. Transcranial magnetic stimulation in the investigation and treatment of schizophrenia: a review. *Schizophr Res* 2004;71:1–16.

- Houdayer E, Degardin A, Cassim F, Bocquillon P, Derambure P, Devanne H. The effects of low- and high-frequency repetitive TMS on the input/output properties of the human corticospinal pathway. *Exp Brain Res* 2008;187(2):207–17.
- Kammer T, Beck S, Thielscher A, Laubis-Herrmann U, Topka H. Motor thresholds in humans: a transcranial magnetic stimulation study comparing different pulse waveforms, current directions and stimulator types. *Clin Neurophysiol* 2001;112:250–8.
- Krnjevic K, Randic M, Straughan DW. An inhibitory process in the cerebral cortex. *J Physiol* 1966;184:16–48.
- McConnell KA, Nahas Z, Shastri A, Lorberbaum JP, Kozel FA, Bohning DE, et al. The transcranial magnetic stimulation motor threshold depends on the distance from coil to underlying cortex: a replication in healthy adults comparing two methods of assessing the distance to cortex. *Biol Psychiatry* 2001;49:454–9.
- Moliadze V, Giannikopoulos D, Eysel UT, Funke K. Paired-pulse transcranial magnetic stimulation protocol applied to visual cortex of anaesthetized cat: effects on visually evoked single-unit activity. *J Physiol* 2005;566:955–65.
- Moliadze V, Zhao Y, Eysel U, Funke K. Effect of transcranial magnetic stimulation on single-unit activity in the cat primary visual cortex. *J Physiol* 2003;553:665–79.
- Pascual-Leone A, Rubio B, Pallardo F, Catala MD. Rapid-rate transcranial magnetic stimulation of left dorsolateral prefrontal cortex in drug-resistant depression. *Lancet* 1996;348:233–7.
- Pascual-Leone A, Walsh V, Rothwell J. Transcranial magnetic stimulation in cognitive neuroscience – virtual lesion, chronometry, and functional connectivity. *Curr Opin Neurobiol* 2000;10:232–7.
- Pasley BN, Allen EA, Freeman RD. State-dependent variability of neuronal responses to transcranial magnetic stimulation of the visual cortex. *Neuron* 2009;62:291–303.
- Paus T, Jech R, Thompson CJ, Comeau R, Peters T, Evans AC. Transcranial magnetic stimulation during positron emission tomography: a new method for studying connectivity of the human cerebral cortex. *J Neurosci* 1997;17:3178–84.
- Rilling JK, Insel TR. The primate neocortex in comparative perspective using magnetic resonance imaging. *J Hum Evol* 1999;37:191–223.
- Rizzo V, Siebner HR, Modugno N, Pesenti A, Munchau A, Gerschlagel W, et al. Shaping the excitability of human motor cortex with premotor rTMS. *J Physiol* 2004;554:483–95.
- Rossini PM, Barker AT, Berardelli A, Caramia MD, Caruso G, Cracco RQ, et al. Non-invasive electrical and magnetic stimulation of the brain, spinal cord and roots: basic principles and procedures for routine clinical application. Report of an IFCN committee. *Electroencephalogr Clin Neurophysiol* 1994;91:79–92.
- Roth Y, Amir A, Levkovitz Y, Zangen A. Three-dimensional distribution of the electric field induced in the brain by transcranial magnetic stimulation using figure-8 and deep H-coils. *J Clin Neurophysiol* 2007;24:31–8.
- Ruff CC, Driver J, Bestmann S. Combining TMS and fMRI: from 'virtual lesions' to functional-network accounts of cognition. *Cortex* 2009;45:1043–9.
- Strafella AP, Paus T, Barrett J, Dagher A. Repetitive transcranial magnetic stimulation of the human prefrontal cortex induces dopamine release in the caudate nucleus. *J Neurosci* 2001;21:RC157.
- Strafella AP, Vanderwerf Y, Sadikot AF. Transcranial magnetic stimulation of the human motor cortex influences the neuronal activity of subthalamic nucleus. *Eur J Neurosci* 2004;20:2245–9.
- Tofts PS. The distribution of induced currents in magnetic stimulation of the nervous system. *Phys Med Biol* 1990;35:1119–28.
- Walsh V, Cowey A. Transcranial magnetic stimulation and cognitive neuroscience. *Nat Rev Neurosci* 2000;1:73–9.